

VISIBLE SPECTROSCOPY OF METHYLENE BLUE ON HECTORITE, LAPONITE B, AND BARASYM IN AQUEOUS SUSPENSION

J. CENENS AND R. A. SCHOONHEYDT

Laboratorium voor Oppervlaktechemie, Katholieke Universiteit Leuven
Kardinaal Mercierlaan 92, B-3030 Leuven (Heverlee), Belgium

Abstract—The absorption spectra of methylene blue ion exchanged on hectorite, Laponite B, Barasym, or sepiolite in dilute aqueous suspensions show the presence of the monomer, the protonated monomer, the dimer, and the trimer. Due to conformational differences, the absorption band maximum of the monomer with respect to its maximum in aqueous solution is red shifted when it is adsorbed on the external surface and blue shifted when it is adsorbed on the interlamellar surface. The availability of the interlamellar surface for methylene blue as a function of the type of clay and/or the counterion present thereby can be probed. The results indicate that 0.6–0.7% of the cation-exchange capacity of Barasym consists of acid sites capable of protonating methylene blue. Counterions of low hydration energy were found to induce a small number of similar sites in hectorite and Laponite B; hence, these sites must be situated on the external surface. Dimers formed on external surfaces show one absorption band. Dimers formed on the interlamellar surface of hectorite yield spectra having two absorption bands. The trimer was formed only at the external surface. With increasing loading of the clays, the spectra of methylene blue showed metachromasy. The metachromatic behavior can be fully explained by dye aggregation, which is the result of its concentration on the surface. No π -electron interaction with the surface oxygens need be invoked.

Key Words—Adsorption, Barasym, Hectorite, Laponite, Methylene blue, Sepiolite, Visible spectroscopy.

INTRODUCTION

The techniques of photochemistry and photophysics have been intensively applied to the study of interfaces, both organic (micelles, membranes, polymers) and inorganic (silica, alumina, zeolites, clays). A general review of the methods and materials was given by Thomas (1984, 1987). For organic molecules on clays, luminescence spectroscopy is a useful technique because of its extremely high sensitivity and because dynamic processes can be studied. The disadvantage of luminescence spectroscopy is its restriction to luminescent molecules on clays that are essentially free of Fe^{3+} (Schoonheydt *et al.*, 1984, 1986; Cenens *et al.*, 1987; Viaene *et al.*, 1987). Moreover, interpretation of the results is hampered by the heterogeneity of the clay minerals themselves and by side reactions of the organic probe, such as protonation and aggregation.

Methylene blue (MB) is a cationic dye (Figure 1), which forms face-to-face dimers in dilute aqueous solutions and higher aggregates at increasing dye concentration (Fornili *et al.*, 1981). The dye is sensitive to changes in the polarity of its surroundings (Handa *et al.*, 1983). A summary of its spectral properties is given in Table 1. The adsorption of MB is useful in determining the cation-exchange capacity and the surface area of clay minerals and in differentiating montmorillonites from illites or kaolinites in mixtures (Pham Thi Hang and Brindley, 1970; Taylor, 1985).

Bergmann and O'Konski (1963) were the first to give a detailed spectroscopic account of MB adsorption on Na-montmorillonite. The intensity of the monomer

band, at 670 nm, rapidly decreased with increasing loading, and at shorter wavelengths new bands, at 605 and 579 nm, gained intensity. Such a shift of the most important absorption band to shorter wavelengths has been observed with many concentrated dye solutions, and is generally called metachromasy (Michaelis and Granick, 1945; Schubert and Levine, 1955). Because the observed band positions were identical to those of concentrated dye solutions, Bergmann and O'Konski (1963) concluded that dimers and even higher polymers were formed on the surface of montmorillonite. The presence of dimers even at small loadings was explained by the hypothesis that special sites existed that had a strong preference for dimers.

Yariv and Lurie (1971) also observed metachromasy of MB on Wyoming bentonite. Because the observed $d(001)$ value was only 13.5 Å, they ascribed the metachromasy to the interaction of the lone pair of electrons of the surface oxygens with the π electrons of the dye. The same observation and interpretation was put forward for acridine orange (Cohen and Yariv, 1984). Grauer *et al.* (1984), however, did not detect metachromasy with rhodamine 6G because the $\text{C}_6\text{H}_5\text{COOC}_2\text{H}_5$ substituent of rhodamine 6G hampered an efficient interaction between the oxygens and the π electrons (the formulae of the dyes are given in Figure 1).

The phenomenon of metachromasy has been described also for proflavine, and Cenens *et al.* (1987) agreed with Bergmann and O'Konski that it was due to surface aggregation of the dye molecules which were

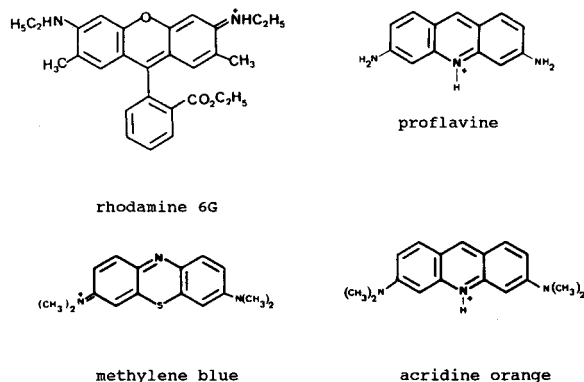


Figure 1. Structural formulae of the dye molecules.

concentrated in a very small volume around the clay particles. The aim of the present paper is to substantiate this conclusion and to see if information, similar to that obtained by luminescence techniques (Schoonheydt *et al.*, 1984, 1986; Cenens *et al.*, 1987; Viaene *et al.*, 1987), can be obtained by classical absorption spectroscopy using MB as a probe molecule.

EXPERIMENTAL

Preparation of the clays

Hectorite and Barasym, from the Source Clays Repository of the Clay Minerals Society, sepiolite from Tolsa SA (Madrid, Spain), and Laponite B from Laporte Industries (United Kingdom) were used. Barasym is a synthetic 2:1 phyllosilicate having a random layering of expandable and non-expandable dioctahedral layers (Wright *et al.*, 1972). The ratio of non-expandable to expandable layers is 2 to 1 (van Olphen and Fripiat, 1979). Only the sites on the external surface and those situated on the swelling layers are easily accessible for exchange. Hectorite is a trioctahedral montmorillonite (Grim, 1953). Laponite B is a synthetic hectorite of small particle size (200–300 Å, van Olphen and Fripiat, 1979). Sepiolite is a non-expandable clay mineral containing 9.6×10.6 Å structural channels (Alvarez, 1984). These clays have significantly different external surfaces (Table 2) and low iron contents.

The clays were saturated with Na^+ by repeated (three times) exchange with 1-mole/dm³ NaCl solutions. The <2- μm fraction was separated, concentrated in 1-mole/dm³ NaCl, and stored in the dark at 277 K to minimize bacterial growth. Stable suspensions suitable for spectroscopic studies were prepared by dialyzing the stock suspension until they were salt-free, and separating the <0.3- μm fraction by centrifugation. The clay content was about 5 g/dm³. The Laponite B sample was not fractionated, because of its small particle size. Cation-exchange capacities (CEC) of these fractions (Table 2) were measured using the ²²Na-method (Peigneur *et al.*, 1975). The value for Barasym was much lower than expected from the charge density of the layers. The ammonium ions which compensated the charges in the non-expandable layers (van Olphen and Fripiat, 1979) were not accessible for exchange with Na^+ ions. Samples of hectorite and Laponite B having different counterions (K^+ , Cs^+ , NH_4^+ , Mg^{2+} , and Ca^{2+}) were prepared by exchanging desalted Na-clay with the desired Cl-salt, and dialyzing until no Cl^- was detected (AgCl test).

Preparation of the dye-clay samples

Dye-clay suspensions were prepared by shaking overnight 0.01 dm³ of an aqueous 10^{-5} mole/dm³ solution of MB with

Table 1. Band positions (λ) and extinction coefficients (ϵ) of methylene blue.

Species	In aqueous solution		Adsorbed on clays	
	λ (nm)	ϵ (dm ³ /mole·cm)	λ (nm)	ϵ (dm ³ /mole·cm)
MB ⁺	664	95,000 (1)	653	100,000
			673	116,000
MBH ²⁺	741	76,000 (2)	763	86,000
(MB ⁺) ₂	605	132,000 (1)	596	80,000
(MB ⁺) ₃	580	110,000 (3)	697	22,000 (1)
			570	114,000

(1) Bergmann and O'Konski (1963); (2) Lewis and Bigelsen (1943); (3) Braswell (1968).

0.03 dm³ of the clay suspensions, containing the appropriate amount of clay to obtain the desired loading. The final dye concentration was always 2.5×10^{-6} mole/dm³. Loadings are herein expressed as a percentage of the CEC values given in Table 2. Buffered suspensions were prepared by adding 0.01 dm³ of a dilute (0.001 mole/dm³) buffer solution ($\text{CH}_3\text{COONa}/\text{CH}_3\text{COOH}$ for pH 4 or $\text{NaOH}/\text{NaHCO}_3$ for pH 9) instead of 0.01 dm³ H₂O. Because the dye concentration was constant (2.5×10^{-6} mole/dm³), extremely small loadings were realized by a high concentration of clay in the suspension. This was easiest to realize for Laponite B. Indeed, the average particle size of the clays (Table 2) was smaller than the wavelength of recording (800–500 nm). Therefore, light scattering decreased with decreasing particle size (Kortum, 1969). On the other hand, Laponite B was also the only clay that formed stable aqueous suspensions with 100% loading of methylene blue. For hectorite and Barasym, the maximum loading to avoid flocculation was 20–25%. All manipulations were done in polyethylene vessels (because MB adsorbs on glass surfaces) and in the dark to minimize photochemical degradation of MB. The adsorption of MB was checked by centrifugation of the clay suspensions at 20,000 g during 30 min or by dialyzing against a known amount of distilled water. The supernatant and the equilibrium dialysate were checked for residual methylene blue by UV-VIS spectroscopy. For Laponite B, Barasym, and hectorite samples the adsorption was quantitative for all loadings investigated. On sepiolite the adsorbed MB was always in equilibrium with MB in solution and adsorption was not quantitative.

Methylene blue (100%) from UCB (Belgium) was used as received. The spectral properties were similar to those reported in the literature (Table 1).

Spectroscopy

Absorption spectra of MB-clay suspensions and identical MB-free clay suspensions were taken in the range 800–500 nm against pure water with a Cary 17 instrument connected to a HP 9825B desktop computer. The spectra of the pure clays were subtracted from those of the corresponding MB-

Table 2. N₂-surface areas, ²²Na-cation-exchange capacity (CEC), and particle diameter of the clays.

Clay	Surface area (m ² /g)	CEC ($\mu\text{mole/g}$)	Diameter (Å)
Hectorite	63 (1)	526	3000
Barasym	133 (1)	464	1000 (1)
Laponite B	360 (1)	568	300 (1, 2)
Sepiolite	276 (3)	200 (4)	—

(1) van Olphen and Fripiat (1979); (2) Avery and Ramsay (1986); (3) Alvarez (1984); (4) Cenens *et al.* (1987).

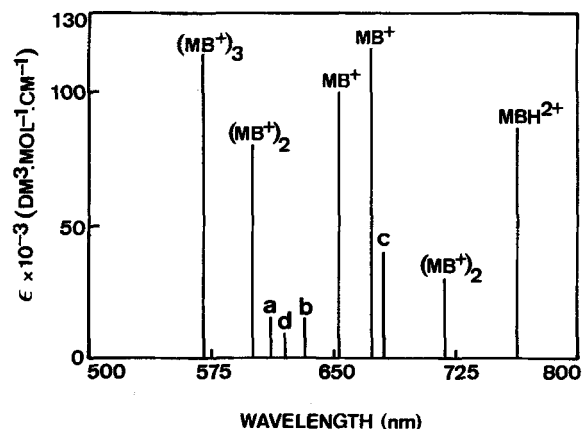


Figure 2. Schematic presentation of the different band positions of methylene blue adsorbed on clays. The height of the lines equals the extinction coefficients given in Table 1, except for the 0-1 vibronic component of MB^+ (a) and the MB^+ form absorbing at 632 nm (b), for which no ϵ -values have been determined. Lines c and d represent the 0-1 and 0-2 vibronic components of MBH^{2+} , respectively.

clay materials to obtain the spectra of adsorbed MB only. By this subtraction the background due to light scattering of the clay particles was eliminated.

RESULTS

Four different MB species were found on the clays: the monomer (MB^+), the protonated monomer (MBH^{2+}), the dimer ($(\text{MB}^+)_2$) and the trimer ($(\text{MB}^+)_3$). These species were also present in aqueous solution. In water the 0-0 band of the monomer adsorbed at 664 nm, with a molar extinction coefficient ϵ of 95,000 $\text{dm}^3/(\text{mole} \cdot \text{cm})$; a shoulder at 610 nm was identified as the corresponding 0-1 vibronic transition (Bergmann and O'Konski, 1963). According to Lewis and Bigeleisen (1943), the pK_a of MBH^{2+} is 0.5 and MB^+ is completely protonated only in a 3 N H_2SO_4 solution. Under these conditions the absorption maximum is at 741 nm with a second maximum at 678 nm and a shoulder at ~ 615 nm. These maxima represent the vibronic components of MBH^{2+} and have relative intensities of 1, 0.52, and 0.17, respectively (Lewis and Bigeleisen, 1943). The 741-nm band has an ϵ value of 76,000 $\text{dm}^3/(\text{mole} \cdot \text{cm})$. By increasing the dye concentration dimers were formed, which produced bands at 605 nm ($\epsilon = 132,000 \text{ dm}^3/(\text{mole} \cdot \text{cm})$) and at ~ 697 nm ($\epsilon = 22,000 \text{ dm}^3/(\text{mole} \cdot \text{cm})$) (Bergmann and O'Konski, 1963). A further increase of the concentration led to trimerization; one band was noted at ~ 580 nm ($\epsilon = 110,000 \text{ dm}^3/(\text{mole} \cdot \text{cm})$) (Braswell, 1968). The spectra of the dye aggregates were very difficult to obtain in solution due to the high dye concentrations necessary to observe them.

The positions of the band maxima and the corresponding ϵ values of the four species on the surface of clay minerals are given in Table 1. The positions of

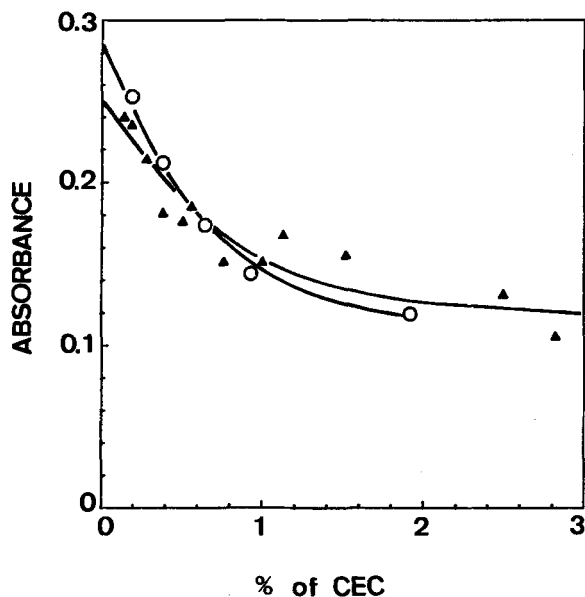


Figure 3. Variation of the MB^+ absorbance with the loading on: (O) Barasym at 673 nm (pH 9); (\blacktriangle) Na-hectorite at 653 nm (pH 7).

the band maxima of each species are summarized in Figure 2 and were taken at that loading where they dominated the spectrum. The ϵ values were obtained by plotting the absorbance values of the species against the loading (expressed as % of CEC). Examples for MB^+ and $(\text{MB}^+)_3$ are shown in Figures 3 and 4. The absorbance values of the monomeric species decreased with the loading due to dye aggregation, and the true ϵ values are obtained by extrapolating to 0% loading and dividing the so-obtained absorbance values by the constant dye concentration of $2.5 \times 10^{-6} \text{ mole}/\text{dm}^3$.

The $(\text{MB}^+)_3$ absorbance attained a maximum at high loadings. This maximum absorbance divided by the dye concentration of $2.5 \times 10^{-6} \text{ mole}/\text{dm}^3$ and multiplied by 3 gives the exact ϵ . This procedure worked

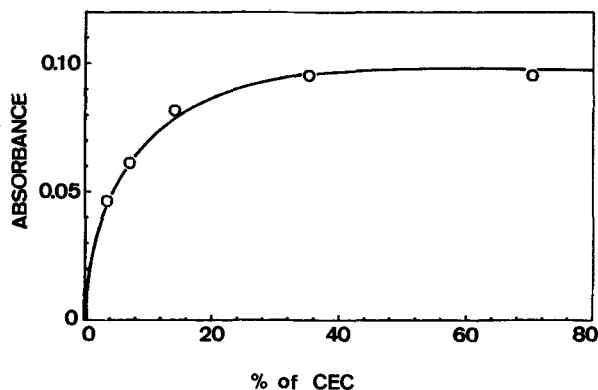


Figure 4. Variation of the $(\text{MB}^+)_3$ absorbance on Na-La-ponite at 570 nm with the loading.

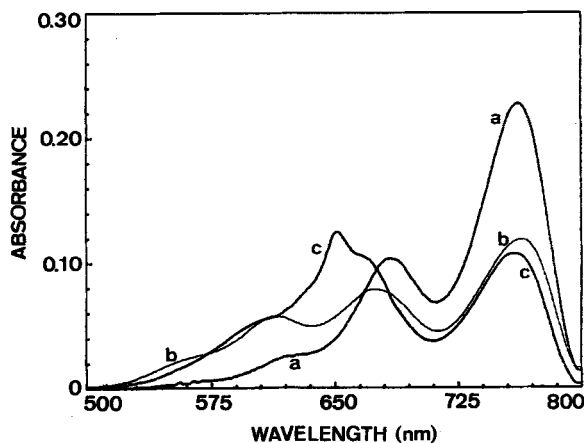


Figure 5. Absorption spectra of methylene blue on: (a) Barasym, 0.2%, pH 4; (b) Barasym, 2.0%, pH 4; and (c) Na-hectorite, 0.3%, pH 4.

well for all the species except $(MB^+)_2$, probably because the dimer band at ~ 600 nm was never "pure," but contained contributions from MB^+ and $(MB^+)_3$.

On the clays MB^+ has four characteristic bands with maxima at 673, 653, 632, and 611 nm. Not all of them can be accounted for as vibrational fine structure bands, because the differences in frequency are too small and because the intensity ratios depend on the experimental conditions. They always occur in pairs: 673 nm–611 nm and 653 nm–632 nm (shoulder). The ϵ value at 673 nm was found to be $116,000 \text{ dm}^3/(\text{mole}\cdot\text{cm})$ (Figure 3). MBH^{2+} showed vibronic structure, with components at 763 ($\epsilon = 86,000 \text{ dm}^3/(\text{mole}\cdot\text{cm})$), 683, and 620 nm. For $(MB^+)_2$ two bands can be distinguished: one at ~ 600 nm and one weak band at 718 nm. The last band was only seen with hectorite. The trimer is the only species that showed only one band, which is at 570 nm ($\epsilon = 114,000 \text{ dm}^3/(\text{mole}\cdot\text{cm})$) (Figure 4). The similarity of this value to that of the monomer was

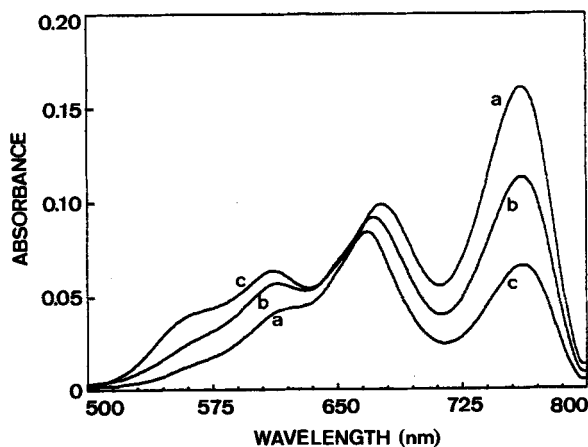


Figure 6. Absorption spectra of methylene blue in neutral suspensions (pH 7) of Barasym: (a) 0.4%; (b) 1.0%; (c) 1.9%.

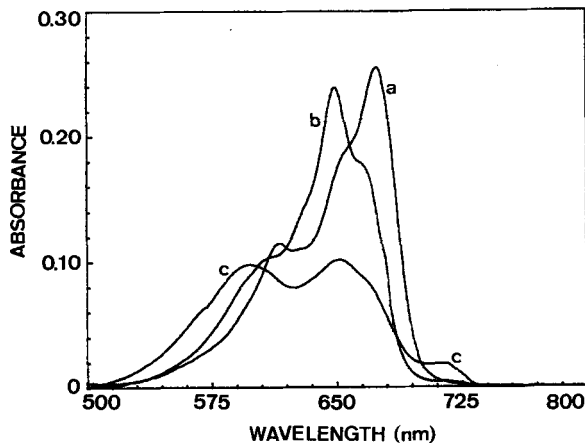


Figure 7. Absorption spectra of methylene blue at pH 9 on: (a) Barasym, 0.2%; (b) Na-hectorite, 0.1%; (c) Na-hectorite, 2.8%.

expected, because the trimer consists of three monomers, all of which are equally capable of absorbing light (Cantor and Schimmel, 1981). A description of these bands as a function of the type of clay and the experimental conditions follows.

Barasym

Spectra of MB on Barasym at different loadings and different pH values are shown in Figures 5–7. At pH 4 (Figure 5) and the smallest loading investigated (0.2%), the spectrum was that of MBH^{2+} , red-shifted by 22 nm with respect to the solution spectrum. The 0–0 band was at 763 nm ($\epsilon = 86,000 \text{ dm}^3/(\text{mole}\cdot\text{cm})$), the 0–1 and the 0–2 bands were at 683 and 620 nm, respectively, and had relative intensities of 1.0, 0.46, and 0.11. With increasing loading the bands at 683 and 620 nm shifted to the blue due to MB^+ absorption and $(MB^+)_2$ absorption, respectively. The intensity of the 763-nm band of MBH^{2+} decreased relative to the intensities of the other bands, and the 570-nm band of $(MB^+)_3$ became apparent (Figure 5).

The same overall spectra were recorded for neutral samples (pH 7) (Figure 6), except that the intensities of the MBH^{2+} bands were less pronounced. The monomer became apparent and had a characteristic absorption at 673 nm. At the highest loading investigated (18.2%) the MBH^{2+} bands completely disappeared, the MB^+ and $(MB^+)_2$ bands were strongly reduced, and the $(MB^+)_3$ band dominated the spectrum (trimer spectra are shown in Figures 9–11).

At pH 9 the surface of Barasym contained no MBH^{2+} (Figure 7); however, two MB^+ absorption bands at 673 and 653 nm were clearly present in the spectra, plus a second, relatively sharp maximum at 611 nm, which was likely the 0–1 vibronic transition of MB^+ and its 0–0 band at 673 nm. As the loading increased the 615- and the 570-nm bands increased in relative intensity. The former was a superposition of the dimer band and

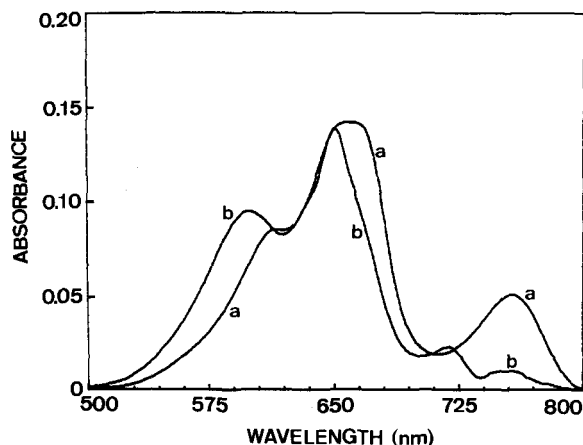


Figure 8. Absorption spectra of methylene blue in neutral suspensions (pH 7) of: (a) Cs-hectorite, 0.8%; (b) Mg-hectorite, 0.4%.

the 0–1 vibronic transition of MB^+ at 611 nm. The latter was the trimer band.

Hectorite

MB^+ on hectorite in aqueous suspension was studied at different pHs and in the presence of different counterions. The spectra of MB on Na-hectorite suspensions at pH 9 (Figure 7) showed the following features. The most intense band was that of MB^+ at 653 nm, with $\epsilon = 100,000 \text{ dm}^3/(\text{mole} \cdot \text{cm})$ (Figure 3). The MB^+ species absorbing at 673 nm was present as a shoulder. The intensity ratio 653:673 was the reverse of that of Barasym. Two features not seen in the spectra of MB on Barasym were present: a weak shoulder at 632 nm and a weak band at 718 nm. By increasing the loading, the MB^+ bands decreased, whereas that of $(\text{MB}^+)_2$ at $\sim 600 \text{ nm}$ intensified, shifted gradually to shorter wavelengths, broadened, and became the most important at loadings $> 7.6\%$. The highest ϵ value found was $\sim 80,000 \text{ dm}^3/(\text{mole} \cdot \text{cm})$ at 596 nm. The 718-nm absorption increased in proportion to the $(\text{MB}^+)_2$ band and was interpreted as a second $(\text{MB}^+)_2$ band. The position of this second band was predicted theoretically (see Appendix). The absence of a resolved band at 570 nm indicated a lack of trimerization. The spectra for the neutral suspensions (pH 7) were similar to those at pH 9, but a weak band at 760 nm indicated the presence of some MBH^{2+} . The latter band was clearly visible at pH 4, although not to the extent noted for Barasym (Figure 5).

Changing the counterion affected the spectra significantly (Figure 8). Qualitatively, the spectra of MB on Ca- and Mg-hectorite were similar to that of MB on Na-hectorite. For Cs^+ , NH_4^+ , and K^+ the following changes were apparent from Figure 8: (1) an increase of the MBH^{2+} band at 763 nm with respect to that of Na-hectorite; (2) the 673- and 653-nm MB^+ bands were similar in intensity; therefore these samples appeared

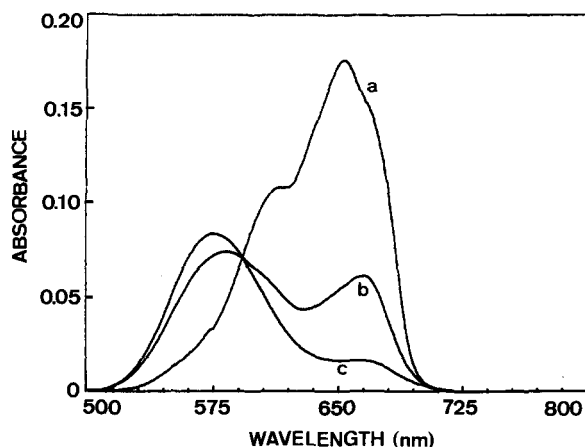


Figure 9. Absorption spectra of methylene blue in neutral (pH 7) Na-Laponite suspensions: (a) 0.2%; (b) 14.1%; (c) 70.4%.

to be intermediate between those of Barasym and Na-hectorite; (3) the 611-nm band was sharper than in the spectra of Na-hectorite. This and the absence of the 718-nm dimer band were taken as indications that the 611-nm band was mainly due to the 0–1 vibronic component of the 673-nm band.

For the same loading (0.8%) the extent of protonation, measured by the intensity of the 763-nm band, was in the order $\text{NH}_4^+ > \text{Cs}^+ > \text{K}^+ > \text{Ca}^{2+} > \text{Mg}^{2+} > \text{Na}^+$ for unbuffered suspensions (pH 7).

Laponite B

Laponite suspensions were studied as a function of the counterion (Na^+ , Ca^{2+} , Cs^+ , and K^+). The spectra of methylene blue on Na-Laponite are shown in Figure 9. The main band at 653 nm had shoulders at 673 and 632 nm. The bands were broad and poorly resolved. The results for Barasym and hectorite suggested that these bands are all monomer bands. As the loading

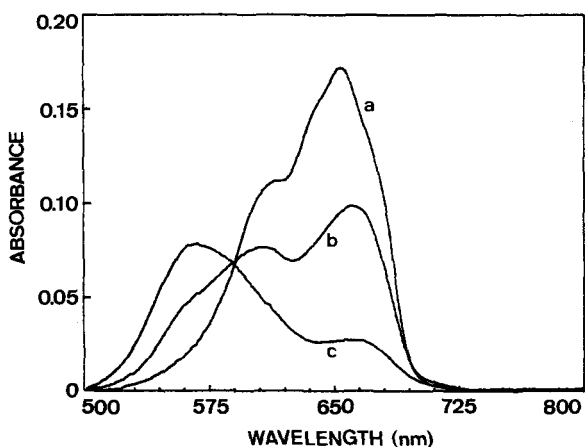


Figure 10. Absorption spectra of methylene blue in neutral (pH 7) Ca-Laponite suspensions: (a) 0.2%; (b) 1.4%; (c) 23.5%.

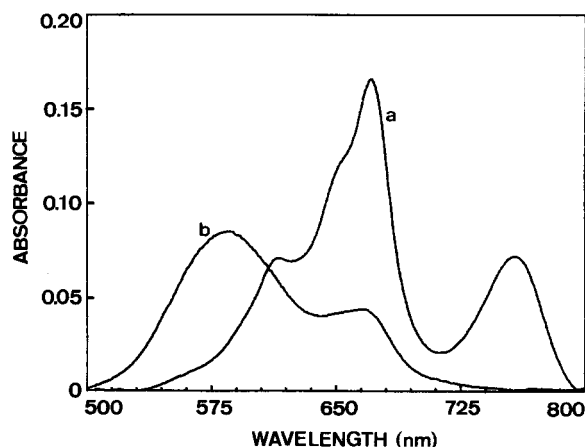


Figure 11. Absorption spectra of methylene blue on K-Laponite: (a) 0.2%, pH 7; (b) 23.5%, pH 9.

increased, the monomer bands and the dimer band at 610 nm decreased in intensity, and the trimer band at 570 nm gained intensity to become the most important band at high loadings. The spectra of Ca-Laponite were similar (Figure 10), but trimerization set in at smaller loadings.

On neutral suspensions of K-Laponite (pH 7), protonation was clearly visible at small loadings by the MBH^{2+} band at 763 nm, but the MB^+ band at 673 nm was the most intense absorption band (Figure 11). A clear sharp band was noted at 611 nm. As for Barasym, Cs- and K-hectorite, this 611-nm band was mainly due to the 0-1 vibronic component of the 673-nm MB^+ absorption. If protonation is taken into account, this spectrum was similar to those of MB on Barasym. The spectra of MB on Cs-Laponite (Figure 12) were the same as those of MB on K-Laponite, except for the absence of protonation, in contrast with the spectra of Cs-hectorite (pH 7).

Dye aggregation was dependent on the counterion.

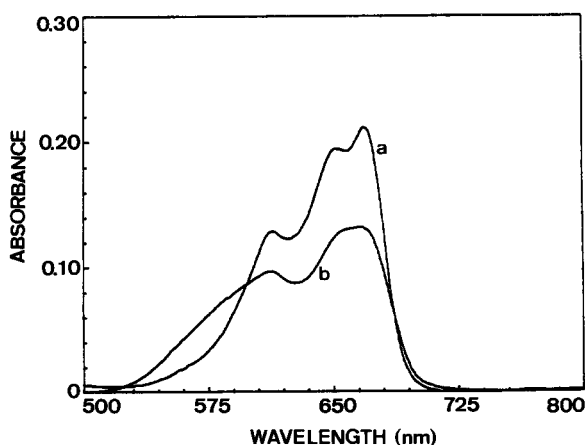


Figure 12. Absorption spectra of methylene blue in neutral (pH 7) Cs-Laponite suspensions: (a) 0.2%; (b) 23.5%.

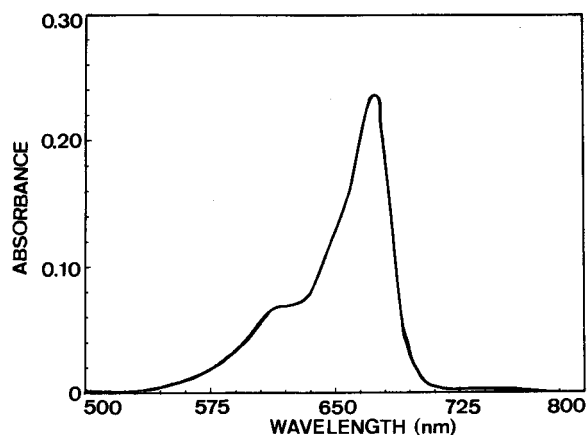


Figure 13. Absorption spectrum of methylene blue on sepiolite (2%, pH 7).

With Cs^+ the trimer band was only a shoulder, whereas the monomer bands retained considerable intensity (Figure 12). High loadings on Ca-, Na- and K-Laponite (>20%) produced the trimer band at 570 nm with an ϵ value of $114,000 \text{ dm}^3/(\text{mole} \cdot \text{cm})$ and some residual MB^+ , which adsorbed at $\sim 660 \text{ nm}$ (Figures 9-11).

Sepiolite

The adsorption of methylene blue on sepiolite was not quantitative; only low loadings could be investigated without significant contribution to the absorbance from methylene blue in solution. The most intense absorption was at 673 nm (MB^+) with a shoulder at 610 nm ($(\text{MB}^+)_2$ and 0-1 transition of MB^+) (Figure 13). By increasing the dye content both these bands decreased in intensity, and a shoulder appeared at 570 nm ($(\text{MB}^+)_3$). The shoulder at 653 nm was very weak, and no bands were noted at 632 nm, nor was a band noted at about 718 nm. Only a very small amount of MBH^{2+} was visible (Figure 13).

DISCUSSION

When MB comes in contact with clays four reactions occur: ion exchange, protonation, dimerization and trimerization. The relative amounts of these four forms of MB depend not only on the loading but also on the type of clay and for each clay, on the type of exchangeable cation. Interestingly, two distinct types of MB^+ were found, each with a characteristic absorption in the visible (673 and 653 nm), and each with relative amounts that are dependent on the type of clay and the type of exchangeable cation. Therefore, MB is an excellent fingerprint molecule to probe surface properties of clays in aqueous suspensions.

Surface reactions

When MB exchanges on clays in aqueous suspension the distribution of the molecules depends on:

(1) The available surface area, which in turn, depends on three factors: particle size, the swelling of the clay, and the type of exchangeable cation. If the particle size decreases, the external surface area increases and so does the number of external surface sites for adsorption of MB. An extreme case is Laponite, however, Barasym also consists of small particles, at least as is indicated by the N_2 -BET surface area (Table 2). In water, clays are not completely swollen, but form tactoids (Fripiat *et al.*, 1984). The replacement of Na^+ with large monovalent cations such as K^+ , Cs^+ , and NH_4^+ , which have small hydration power, leads to larger tactoids (or the number of individual clay platelets per tactoid increases), and the spacing between the clay platelets in the tactoid becomes smaller (Rausell-Colom and Serratos, 1987). The spacings reported for these cations range from 12 Å for Cs-montmorillonite (independent of the water content) to 15 Å for K-montmorillonites (Newman, 1987). Clays saturated with divalent cations (Ca^{2+} , Mg^{2+}) also form tactoids easily and allow three layer hydrates to be formed in the interlamellar space. Divalent cations all give a spacing of 19 Å when immersed in water but do not swell any further as Na- and Li-clays do (Newman, 1987).

(2) Finally, the distribution of MB over the clay surface depends on the properties of MB itself. In water it easily forms dimers even at concentrations as low as 10^{-5} mole/dm³. Our suspensions all had the constant concentration of 2.5×10^{-6} mole/dm³. Only the monomer MB^+ was then present in solution and exchanged on the clays. MB is concentrated on a clay in a small space around the clay particles. Whether it aggregates in that space or not, depends on the adsorptive power of the sites on the surface relative to the driving force for aggregation. If the complete surface area of 750 m²/g is available and if MB is confined in a 10-Å-thick layer around the clay particles, MB is concentrated from solution into a volume which is 267 times smaller. The concentration increases from 2.5×10^{-6} to 6.67×10^{-4} mole/dm³, a value at which extensive dimerization occurs in aqueous solution. By analogy, aggregation should also occur on the surface.

Protonation. The present results indicate that (1) the most acidic clay is Barasym in terms of Bronsted acid sites able to protonate MB^+ in aqueous suspension; (2) the same type of acidity is present to a small extent on hectorite and K-Laponite; and (3) these acid sites are the most selective sites; if they are present, the first molecules of MB^+ reaching the surface protonate. Therefore, protonation is most prevalent at the smallest loadings. For $\epsilon = 86,000$ dm³/(mole · cm), the amount of MBH^{2+} on Barasym (pH 7) is plotted against the loading in Figure 14. The maximum amount of MBH^{2+} is 0.6–0.7% of the CEC or 1.7 – 2.0×10^{18} sites/g. This number may be compared with 2.4×10^{19} Bronsted sites/g found by Fletcher (1984) after water evacuation

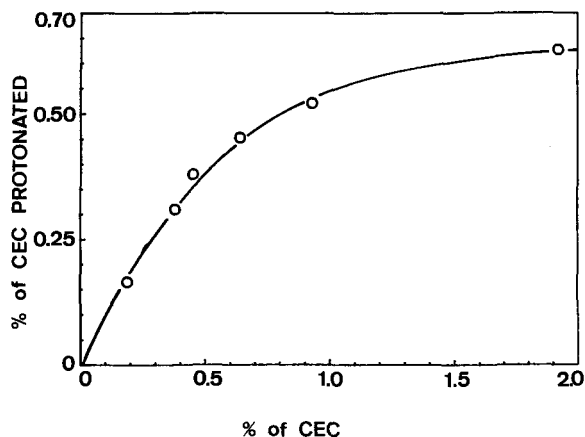


Figure 14. Variation of amount of MBH^{2+} protonated with loading.

(at 373 K), and with 1.5×10^{19} Bronsted sites/g found by Wright *et al.* (1972) on Barasym, treated at 423 K for 1 hr. This difference in the number of sites is not surprising because the present experimental conditions (aqueous suspension and MB with $pK = 0.5$) are not comparable with those of Fletcher (1984) or Wright *et al.* (1972) (dry clay and pyridine with $pK = 4$). Despite these differences, together with the comparable results found for proflavine on Barasym (Cenens *et al.*, 1987), this is probably the first time that the number of acid sites on a clay has been determined quantitatively in aqueous suspension.

As the loading increased, MBH^{2+} disappeared because of aggregation with other dye molecules. The acidity of K-Laponite and NH_4^- , K-, and Cs-hectorite in unbuffered suspensions (pH 7) is puzzling. These clays were swollen only slightly, if at all. The sites which contributed to the acidity were probably: (1) hydroxyl groups on the edges of the platelets (tactoids of individual clay platelets were apparently necessary to generate them); or (2) due to the increased dissociation of water molecules, surrounding cations, which were only partly or not shielded by a hydration shell.

Monomer adsorption. MB molecules are so strongly adsorbed that they adsorb onto the first site of encounter, irrespective of the adsorptive strength of that site. Sites on the external surface are therefore always available for adsorption. Sites on the interlamellar surface are available for MB if the clay contains at least three water layers between the platelets of the tactoid. At such a hydration level, the number of interlamellar sites exceeds the number of external surface sites and, statistically, more MB molecules will adsorb on the interlamellar sites at constant MB concentration than on the external surface sites. On the contrary, if no interlamellar sites are present or if a penetration barrier exists for reaching the interlamellar sites, the number of external surface sites exceeds the number of avail-

able interlamellar sites and more MB will adsorb on external surface sites than on interlamellar sites, because more sites of the first kind are available. Thus, if MB on interlamellar sites can be distinguished spectroscopically from MB on external surface sites, a method exists by which the dispersion of clay platelets in aqueous suspension can be investigated.

The present results for MB confirm this expectation. On sepiolite, which has only external surface, the monomer, MB^+ , absorbs at 673 nm. Ca- and Na-hectorite and Ca- and Na-Laponite have at least three water layers between the layers (Newman, 1987), and most of the monomers absorb at 653 nm. This band is characteristic for MB^+ on interlamellar sites. (The 653-nm band has a shoulder at 632 nm for which we offer no explanation at this moment.) Barasym, K-, and Cs-Laponite, and to a lesser extent, K-, NH_4 -, and Cs-hectorite produced a pronounced 673-nm band, indicating that the number of external surface sites exceeded the number of available interlamellar sites. Thus, these clays occurred as tactoids, which were either non-swelling or mica-type as was Barasym or contain fewer than three water layers.

Dimerization and trimerization. Dimers were seen on all clays at all loadings, except possibly on the very acidic Barasym (pH 4) at the smallest loadings. These results are indicative of the concentration effect around the particles, discussed above. Dimerization also indicates that the energy of interaction between a specific site and MB^+ did not destroy the MB^+-MB^+ interactions. Dimerization was also noted on the interlamellar surfaces as on the external surfaces. Interlamellar dimer formation means that two layers of MB^+ were formed in the interlamellar space; this is confirmed by measurements of the $d(001)$ spacing of a fully exchanged MB^+ -Laponite (15.5 Å) and of proflavine-adsorbed Camp Berteau montmorillonite and Wyoming bentonite (15.5 Å) (Schoonheydt *et al.*, 1986).

Trimers, which adsorb to give a band at 570 nm, were found only on clays occurring as small particles or which had large external surface areas (Barasym, Laponite, sepiolite). On hectorite, the dimer band shifted to the blue with increasing loading without formation of a new band at 570 nm. These "570-nm" trimers were therefore only formed on the external surface and are indicative of a well-defined molecular stacking, three MB^+ -molecules on top of each other.

Spectroscopy

The band characteristic of MB^+ on the external surface of the clays shifted to the red (673 nm) with respect to the solution spectrum (664 nm); that characteristic of MB^+ on the interlamellar surface shifted to the blue (653 nm). For hectorite, the dimer band in the region 605–595 nm was accompanied by a weak band at 718 nm, but not for the other clays. Only one trimer band

was noted (570 nm). These observations merit explanation.

Monomers. The blue shift (664–653 nm) is probably a solvent effect. Indeed, the same shift was observed in solution, if water was replaced by methanol (Handa *et al.*, 1983), suggesting that the polarity of the hydrated clay surface on which MB^+ was adsorbed equals that of methanol. A similar conclusion was drawn by Maes *et al.* (1980) from the red shift of the charge-transfer band of $\text{Cu}(\text{en})_2^{2+}$ on clay surfaces with respect to aqueous solutions.

For MB^+ , this explanation meets a number of difficulties: (1) because the band position was constant for all the clays investigated, the polarity in the surface region was probably independent of the type of exchangeable cation and the amount of water in the interlamellar region. This situation is difficult to visualize in view of the large differences in hydration power of, for example, Na^+ and Cs^+ . (2) The red shift to 673 nm for MB^+ on the external surface could mean that the polarity of the double layer around the external surface of the clay particles was higher than that of water, but such a situation is hard to visualize.

For these reasons we are inclined to look for an explanation in terms of the conformation of the molecule on different surface sites. The $\pi-\pi^*$ transitions of aromatic molecules shift to the red if the molecule is made more planar, i.e., if the aromaticity is increased. This shift occurs because in that conformation, the number of functional π electrons is maximized (Berlmann, 1970). In the reverse situation, i.e., if the chromophore is made nonplanar, the spectra become more diffuse and are blue-shifted.

According to this view, the conformation of MB^+ is more planar if it is adsorbed on the external surface (red shift), and less planar if it is adsorbed on the interlamellar surface (blue shift), both with respect to its conformation in water. These conformations are probably due to the two $\text{N}(\text{CH}_3)_2$ substituents. Indeed, the lone electron pairs on the nitrogens are part of the aromatic system. If they are tilted out of the aromatic plane by steric hindrance, there should be a blue shift. In the reverse case, the shift is to the red. Conformational calculations are necessary to substantiate these qualitative conclusions and to obtain an idea about the extent of distortion of MB^+ on the interlamellar surface with respect to its conformation on the external surface. Regardless, if the 673-nm band is considered as the 0–0 vibronic transition, the 611-nm band (weak) is the corresponding 0–1 band. The energy difference is 1500 cm^{-1} , which is in the range of that found for similar aromatic systems, such as anthracene (1401 cm^{-1}) (Murrell, 1971).

Dimers and trimers. The simplest theory to account for electronic transitions of dimers and trimers is outlined in the Appendix. For dimers two transitions are

expected, one at higher energy and the other at lower energy than that of the monomer transition, but the energy shifts are equal in both directions. Such shifts were found for MB⁺ on hectorite: the weak 718-nm band was 1386 cm⁻¹ lower in energy than the monomer absorption at 653 nm. The intense high energy dimer band should then have been at 599 nm, in agreement with the experimental band position of 605–595 nm.

The intensity ratio of the two bands depends on the relative orientations of the transition dipole moments of the two chromophores in the dimer (Cantor and Schimmel, 1981). Because the transition moments lie in the plane of the aromatic ring system, the intensity ratio provides information about the orientation of the chromophores in the dimer. In the limit of exact parallel orientation of the two identical chromophores in the dimer, the dimer has a center of symmetry, and the low energy band is forbidden. This parallel orientation can be destroyed by vibrational motion of the chromophores with respect to each other or by the existence of an unsymmetrical structure. Under such circumstances the low energy band is present in the spectrum and has an intensity proportional to the degree of distortion (West and Pearce, 1965).

Thus, on the external surface where MB⁺ has a planar conformation, a dimer can be formed wherein the two chromophores are identical, and the dipole moments are oriented in a parallel fashion with respect to each other. The 718-nm band has zero intensity. On the interlamellar surface where the MB⁺ molecule is somewhat distorted, an unsymmetrical dimer is formed, and the 718-nm band shows up in the spectrum.

The following relations exist between the dimer dipole strengths (D_{oa}^+ and D_{oa}^-) in terms of the monomer dipole strength (D_{oa}) (Cantor and Schimmel, 1981):

$$D_{oa}^+ = D_{oa} + D_{oa}x \cos \theta$$

and

$$D_{oa}^- = D_{oa} - D_{oa}x \cos \theta,$$

where θ is the angle between the transition dipoles involved in the individual electronic absorptions of monomer 1 and monomer 2. As an approximation the absorbance values of the two bands involved at 718 and ~600 nm have been used to estimate the angle between the two transition dipoles D_{oa}^+ and D_{oa}^- . The change in dimer conformation on the interlamellar surface with loading can be followed in Figure 15. The angle between the transition moments of the two monomers attains a value of about 60° for interlamellar dimers on hectorite. Bergmann and O'Konski (1963) estimated a value of 13° for the dimer in aqueous solution.

From the three transitions that are possible in trimers, only the highest energy band at 570 nm was noted. Trimers probably formed on the external surface only because the chromophores were oriented in

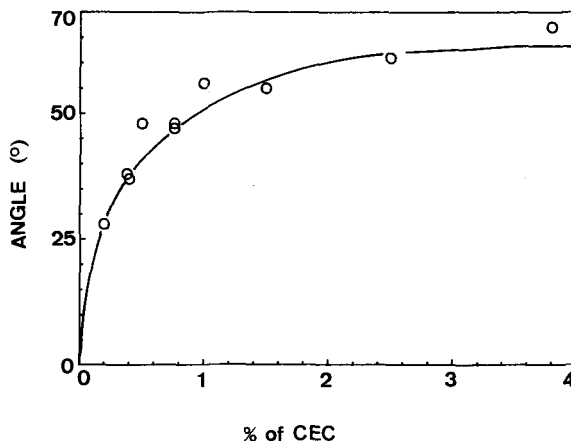


Figure 15. Variation of the angle between the transition dipoles of the two monomers in the dimer with the loading.

an exactly parallel fashion. This is not the case on the interlamellar surface for slightly distorted MB⁺ molecules. The energy difference between the transitions of the trimer and the monomer (673 nm or 14,859 cm⁻¹) is 2685 cm⁻¹. According to the simple theory (Appendix), the dimer should then absorb at 14,859 cm⁻¹ + (2685 cm⁻¹/√2) = 16,758 cm⁻¹ or 597 nm, again in good agreement with experiment.

Thus, the simple theory fully explains the metachromatic effect of dye adsorption on clays in terms of dimerization and trimerization on the surface, exactly as was explained for solution. Ascribing metachromasy to π -electron interactions of MB⁺ with the surface oxygens, as Yariv and Lurie (1971) did, cannot account for the richness of the spectra that were obtained.

SUMMARY AND CONCLUSIONS

Methylene blue is a sensitive fingerprint molecule for probing the surface properties of clays in aqueous suspension. MBH²⁺, two forms of MB⁺, (MB⁺)₂, and (MB⁺)₃ were found on the surface of clays. At small loadings the monomers (MB⁺, MBH²⁺) were the dominant species, but at greater loadings, dimers and trimers were formed at the expense of the monomers. On Barasym at neutral pH, 0.7% of the ²²Na-CEC were present as acid sites, which were able to protonate MB⁺. Acid sites were also present on Laponite and hectorite that had been exchanged with K⁺ or Cs⁺.

On the external surface the MB⁺ absorption spectrum had a maximum at 673 nm, whereas on the interlamellar surface the MB⁺ absorption maximum was at 673 nm. MB⁺ was less planar, thus less aromatic on the interlamellar surface than on the external surface. At small loadings interlamellar adsorption was dominant on Na- and Ca-forms of hectorite and Laponite as determined from the relative intensities of the 653- and 673-nm bands. External surface adsorption was dominant for Barasym, Cs-Laponite and K-Laponite,

whereas K-hectorite and Cs-hectorite were intermediate in behavior.

The dimers on the external surface have one characteristic absorption band at ~ 600 nm, which is due to a parallel alignment of the transition moments in the monomer units. On the interlamellar surface the dimers have two characteristic bands at ~ 600 and 718 nm. From the intensity ratio of those two bands the angle between the transition moments of the two monomers in the dimer can be deduced. It increases with the loading to as much as 60° . Trimers were only seen on external surfaces and yielded one characteristic band at 570 nm. This band is due to the parallel alignment of the three monomers in the trimer.

The dye aggregated at very small loadings. The aggregation was clearly responsible for the observed metachromatic effects, indicating that the distribution of MB^+ molecules over the surface was determined not only by the electrostatic interaction between the negatively charged exchange sites and MB^+ (promoting more or less random adsorption), but also by dye-dye interactions. Because of the formation of dimers and trimers, the use of methylene blue for the determination of surface areas is questionable, especially for clays having a large external surface on which $(MB^+)_3$ is rapidly formed.

ACKNOWLEDGMENTS

Acknowledgment is made to the National Fund of Scientific Research (Belgium) for support of this research and for the research tenure to R.A.S. as Research Director. J.C. thanks the "Instituut voor Aanmoediging van het Wetenschappelijk Onderzoek in Nijverheid en Landbouw (Belgium)" for a Ph.D. grant. The authors thank Laporte Industries for their donation of the Laponite B sample and Tolsa SA for the gift of sepiolite.

APPENDIX

The theory of the spectral properties of dye aggregates was given by Cantor and Schimmel (1981) for a dimer, and is summarized below, together with that for a trimer.

Let Φ_{10} , Φ_{20} , and Φ_{30} represent the electronic ground state of the interacting monomers, and let their excited states be represented by Φ_{1a} , Φ_{2a} , and Φ_{3a} . Now let the monomers in a dimer and a trimer be close enough to interact electronically. If the wave functions of the monomers do not overlap, electron exchange between the monomers can be neglected. Thus, the electrons remain localized, but each monomer is perturbed by the electric field of its neighbor(s) in the aggregate. The Hamiltonian then becomes

$$H = H_1 + H_2 + V_{12}$$

for the dimer and

$$H = H_1 + H_2 + H_3 + V_{12} + V_{23} + V_{13}$$

for the trimer,

(1)

where H_1 , H_2 , and H_3 represent the Hamiltonians of the isolated molecules and V_{12} , V_{23} , and V_{13} represent the interaction potentials. Assuming $V_{12} = V_{23} = V$ and neglecting the in-

teraction between the first and the third monomer, these equations become:

$$H = H_1 + H_2 + V$$

for the dimer and

$$H = H_1 + H_2 + H_3 + 2V$$

for the trimer.

(2)

The ground state wave functions for the aggregates are represented by:

$$\Psi_0 = \Phi_{10}\Phi_{20}$$

for the dimer and

$$\Psi_0 = \Phi_{10}\Phi_{20}\Phi_{30}$$

for the trimer.

(3)

Because each monomer can be excited, the excited states are represented by:

$$\Psi_{1a} = \Phi_{1a}\Phi_{20}$$

and

$$\Psi_{2a} = \Phi_{10}\Phi_{2a}$$

for the dimer and

$$\Psi_{1a} = \Phi_{1a}\Phi_{20}\Phi_{30},$$

$$\Psi_{2a} = \Phi_{10}\Phi_{2a}\Phi_{30},$$

and

$$\Psi_{3a} = \Phi_{10}\Phi_{20}\Phi_{3a}$$

for the trimer.

(4)

To compute the electronic states of the dimer and the trimer, the Schrödinger equation must be solved using the Hamiltonians (2). Approximations may be made by letting the interaction V be weak enough so that the ground-state wavefunction is still Ψ_0 and so that the wavefunctions Ψ_{1a} , Ψ_{2a} , and Ψ_{3a} are still good approximations for the excited state of the aggregate. The complete wavefunction as a sum of the contributions from each separate excited state can be calculated from:

$$\Psi = C_1\Psi_{1a} + C_2\Psi_{2a}$$

and

$$\Psi = C_1\Psi_{1a} + C_2\Psi_{2a} + C_3\Psi_{3a},$$

(5)

where C_1 , C_2 , and C_3 are constants to be chosen to minimize the energy.

The linear combinations must satisfy the criteria of normalization and orthogonality and must be stationary. The appropriate set of secular equations (two for the dimer, three for the trimer) can then be obtained and solved. The resulting wavefunctions and the corresponding energies are listed below:

Wave function	Energy
$\Psi_A^+ = \frac{1}{\sqrt{2}} \cdot (\psi_{1a} + \psi_{2a})$	$E_a + E_0 + V$
$\Psi_A^- = \frac{1}{\sqrt{2}} \cdot (\psi_{1a} - \psi_{2a})$	$E_a + E_0 - V$
$\Psi_A^0 = \frac{1}{\sqrt{2}} \cdot (\psi_{1a} - \psi_{2a})$	$E_a + 2E_0$
$\Psi_A^+ = \frac{1}{2} \cdot (\psi_{1a} + (\sqrt{2})\psi_{2a} + \psi_{3a})$	$E_a + 2E_0 + (\sqrt{2})V$
$\Psi_A^- = \frac{1}{2} \cdot (-\psi_{1a} + (\sqrt{2})\psi_{2a} - \psi_{3a})$	$E_a + 2E_0 - (\sqrt{2})V$

Thus, the singly excited states (two for the dimer, three for the trimer) no longer have the same energy. Instead, their energy levels are split. The absorption frequencies of the transitions are given by the difference in energy between the excited state and the ground state (E_0 for the monomer, $2E_0$ for the dimer, and $3E_0$ for the trimer), as follows:

monomer	$h\nu = E_a - E_0;$
dimer	$h\nu^+ = E_a - E_0 + E_v$ and $h\nu^- = E_a - E_0 - E_v;$
trimer	$h\nu^0 = E_a - E_0,$ $h\nu^+ = E_a - E_0 + (\sqrt{2})E_v,$ and $h\nu^- = E_a - E_0 - (\sqrt{2})E_v.$

REFERENCES

- Alvarez, A. (1984) Sepiolite: Properties and uses: Data accompanying the samples of sepiolite, Tolsa SA, Spain.
- Avery, R. G. and Ramsay, J. D. F. (1986) Colloidal properties of synthetic hectorite clay dispersions: *J. Colloid Interface Science* **109**, 448–454.
- Bergmann, K. and O'Konski, C. T. (1963) A spectroscopic study of methylene blue monomer, dimer, and complexes with montmorillonite: *J. Phys. Chem.* **67**, 2169–2177.
- Berlmann, I. B. (1970) On the empirical correlation between nuclear conformation and certain fluorescence and absorption characteristics of aromatic compounds: *J. Phys. Chem.* **74**, 3085–3093.
- Braswell, E. (1968) Evidence for the trimerisation in aqueous solutions of methylene blue: *J. Phys. Chem.* **72**, 2477–2483.
- Cantor, C. R. and Schimmel, P. R. (1981) *Biophysical Chemistry, Part II*: Freeman, San Francisco, 846 pp.
- Cenens, J., Vliers, D. P., Schoonheydt, R. A., and De Schryver, F. C. (1987) Spectroscopic study of the surface chemistry of proflavine on clay minerals: in *Proc. Int. Clay Conf., Denver, 1985*, L. G. Schultz, H. van Olphen, and F. A. Mumpton, eds., The Clay Minerals Society, Bloomington, Indiana, 352–358.
- Cohen, R. and Yariv, S. (1984) Metachromasy in clay minerals. Sorption of acridine orange by montmorillonite: *J. Chem. Soc., Faraday Trans. 1* **80**, 1705–1715.
- Fletcher, J. C. Q. (1984) The acidity of synthetic mica-montmorillonite and its activity for propene oligomerization: Ph.D. thesis, Dept. Chem. Eng., Univ. Cape Town, Republic of South Africa, 238 pp.
- Fornili, S. L., Sgroi, G., and Izzo, V. (1981) Solvent isotope effect in the monomer-dimer equilibrium of methylene blue: *J. Chem. Soc., Faraday Trans. 1* **77**, 3049–3053.
- Fripiat, J. J., Letellier, M., and Levitz, P. (1984) Interaction of water with clay surfaces: in *Clay Minerals: Their Structure, Behavior and Use*, L. Fowden, R. M. Barrer, and P. B. Tinker, eds., The Royal Society, London, 67–79.
- Grauer, Z., Avnir, D., and Yariv, S. (1984) Adsorption characteristics of rhodamine 6G on montmorillonite and Laponite, elucidated from electronic adsorption and emission spectra: *Can. J. Chem.* **62**, 1889–1894.
- Grim, R. E. (1953) *Clay Mineralogy*: McGraw-Hill, New York, 384 pp.
- Handa, T., Ichihashi, C., Yamamoto, I., and Nakagaki, M. (1983) The location and microenvironment of dimerizing cationic dyes in lipid membranes as studied by means of their absorption spectra: *Bull. Chem. Soc. Japan* **56**, 2548–2554.
- Kortum, G. (1969) *Reflectance Spectroscopy. Principles, Methods, Applications*: Springer-Verlag, Berlin, 366 pp.
- Lewis, G. N. and Bigeleisen, J. (1943) Methylene blue and other indicators in general acids. The acidity function: *J. Amer. Chem. Soc.* **65**, 1144–1150.
- Maes, A., Schoonheydt, R. A., Cremers, A., and Uytterhoeven, J. B. (1980) Spectroscopy of $\text{Cu}(\text{en})_2^{2+}$ on clay surfaces. Surface and charge-density effects: *J. Phys. Chem.* **84**, 2795–2799.
- Michaelis, L. and Granick, S. (1945) Metachromasy of basic dyestuffs: *J. Amer. Chem. Soc.* **67**, 1212–1219.
- Murrell, J. N. (1971) *The Theory of the Electronic Spectra of Organic Molecules*: Chapman and Hall, London, 328 pp.
- Newman, A. C. D. (1987) The interaction of water with clay mineral surfaces: in *Chemistry of Clay and Clay Minerals*, A. C. D. Newman, ed., Mineralogical Society, London, 237–274.
- Peigneur, P., Maes, A., and Cremers, A. (1975) Heterogeneity of charge density in montmorillonite as inferred from cobalt adsorption: *Clays & Clay Minerals* **23**, 71–75.
- Pham Thi Hang and Brindley, G. W. (1970) Methylene blue adsorption by clay minerals. Determination of surface areas and cation exchange capacities (Clay-organic studies XVIII): *Clays & Clay Minerals* **18**, 203–212.
- Rausell-Colom, J. A. and Serratos, J. M. (1987) Reactions of clays with organic substances: in *Chemistry of Clays and Clay Minerals*, A. C. D. Newman, ed., Mineralogical Society, London, 371–422.
- Schoonheydt, R. A., Cenens, J., and De Schryver, F. C. (1986) Spectroscopy of proflavine on clays: *J. Chem. Soc., Faraday Trans. 1* **82**, 281–289.
- Schoonheydt, R. A., De Pauw, P., Vliers, D. P., and De Schryver, F. C. (1984) Luminescence of $\text{Ru}(2,2'\text{-bipy})_3^{2+}$ in aqueous clay minerals suspensions: *J. Phys. Chem.* **88**, 5113–5118.
- Schubert, M. and Levine, A. (1955) A qualitative theory of metachromasy in solution: *J. Amer. Chem. Soc.* **77**, 4197–4201.
- Taylor, R. K. (1985) Cation exchange in clays and mudrocks by methylene blue: *J. Chem. Tech. Biotechnol.* **35A**, 195–207.
- Thomas, J. K. (1984) *The Chemistry of Excitation at Interfaces*: ACS Monograph **191**; American Chemical Society: Washington, D.C., 320 pp.
- Thomas, J. K. (1987) Characterization of surfaces by excited states: *J. Phys. Chem.* **91**, 267–276.
- van Olphen, H. and Fripiat, J. J. (1979) *Data Handbook for Clay Minerals and Other Non-Metallic Minerals*: Pergamon Press, New York, 346 pp.
- Viaene, K., Cagui, J., Schoonheydt, R. A., and De Schryver, F. C. (1987) Study of the adsorption on clay particles by means of a fluorescent probe: *Langmuir* **3**, 107–111.
- West, W. and Pearce, S. (1965) The dimeric state of cyanine dyes: *J. Phys. Chem.* **69**, 1894–1903.
- Wright, A. C., Granquist, W. T., and Kennedy, J. V. (1972) Catalysis by layer lattice silicates. I. The structure and thermal modification of a synthetic ammonium dioctahedral clay: *J. Catalysis* **25**, 65–80.
- Yariv, S. and Lurie, D. (1971) Metachromasy in clay minerals. Part I. Sorption of methylene blue by montmorillonite: *Israel J. Chem.* **9**, 537–552.

(Received 14 July 1987; accepted 24 December 1987; Ms. 1725)